

Preparation of cobalt hydroxide and cobalt oxide nanostructures using ultrasonic waves and investigation of their optical and structural properties

R. SHOKRANI-HAVIGH^a, Y. AZIZIAN-KALANDARAGH^{a,b*}

^aDepartment of Physics, University of Mohaghegh Ardabili, P.O. Box 179, Ardabil, Iran

^bDepartment of Engineering Sciences, Sabalan University of Advanced Technologies (SUAT), Namin, Iran

Nanocrystalline cobalt hydroxide and cobalt oxide compounds have been prepared using ultrasound-assisted method and some of their optical and structural properties have been characterized by thermogravimetric analyses (TGA), X-ray diffraction (XRD), scanning electron microscope (SEM), and UV-Visible spectroscopy. The results of thermogravimetric analyses show a sharp change in TGA peak, and the onset of the peak (at 250°C) is transition temperature from hydroxide to oxide of the product. The optical absorption studies show that there are two direct band gaps in Co₃O₄ nanostructures. The XRD patterns of the prepared samples shows formation of pure cobalt oxide in cubic structure and cobalt hydroxide compound in hexagonal structure with average grain sizes are below 30 nm. Surface morphology of the prepared structures shows that the nanoparticles from nearly globular aggregates of microdimensions.

(Received July 4, 2014; accepted April 6, 2017)

Keywords: Cobalt oxide, Cobalt hydroxide, X-ray diffraction, Optical properties, Scanning electron microscopy (SEM)

1. Introduction

The study of semiconductor nanostructured materials is an active area of research in materials science, physics, chemistry, and engineering sciences [1-3]. There are some important applications for semiconductor nanostructured materials in several areas of science and technology such as electronics [4], as solar cell materials [5], in catalysis [6], magnetic storage materials [7], and so forth. Cobalt hydroxide, Co(OH)₂, is a main raw material for lithium ion batteries and a promising candidate for supercapacitors [8,9], that cobalt hydroxide mainly exists in two polymorphic modifications, designated as α - and β -Co(OH)₂. Both forms have a hexagonal layered structure. α -Co(OH)₂ is isostructural with hydrotalcite-like compounds while β -Co(OH)₂ is brucite-like and consists of hydroxyl groups with Co(II) ions occupying octahedral sites [10]. Both hydroxides are very promising materials for various important electrical and electrochemical devices, such as supercapacitors [11], electrocatalysts [12], and electrochromic electrodes [13]. The band gap of cobalt hydroxide semiconductor material is reported around 2.4 eV [14]. Upon thermal treatment around 300°C, for one hour, cobalt hydroxide usually transforms to black tricobalttetroxide (Co₃O₄) [15]. Five polymorphs for cobalt oxide (CoO₂, CoO₃, CoO(OH), Co₃O₄, and CoO) have been reported [16-18]. Cobalt oxide with a valence of more than three is unstable in the natural environment. The most stable cobalt oxide structures are Co₃O₄, and CoO [19]. Co₃O₄ has a cubic spinel crystal structure in which the Co²⁺ ions occupy the tetrahedral sites and the Co³⁺ ions the octahedral sites [20]. Its band gap varies from 1.4 to 1.8 eV [21]. Co₃O₄ is magnetic p-type semiconductor

materials [22], which exhibit weak ferromagnetic behavior in its nanostructured form, whereas, bulk Co₃O₄ show antiferromagnetic behavior [23]. Nanoparticles of Co₃O₄ has a wide range of applications in various fields of industry including anode materials for rechargeable Li-ion battery, catalyst, gas sensors and magnetic materials [24-27], solar energy absorbers [28], and heterogeneous catalysts [29]. Co₃O₄ is stable up to 800°C and decomposes to cobalt oxide CoO above 900°C [30]. CoO nanocrystals display superparamagnetism or weak ferromagnetism, whereas bulk CoO is antiferromagnetic [31, 32]. CoO has an energy bandgap between 2.2 and 2.4 eV [33]. The properties of cobalt hydroxide and cobalt oxide in above application are highly related to the particles size. When the size of a material is reduced to the nanometer length scale change the band gap. With change of the band gap significantly alter the materials physics and chemistry [34]. There are several methods for the preparation of nanoparticle materials including successive ionic layer adsorption (SILAR) [35], sol-gel [36], microwave-assisted preparation [37], chemical vapor deposition [38] hydrothermal method [39] and ultrasound-assisted technique. However, among them, ultrasound-assisted technique is simple and major advantage of this technique is that the shape and size of the nanoparticles can be adjusted by varying the operating parameters which include ultrasonic power, current density, deposition potential and the ultrasonic versus electrochemical pulse times [40]. When an ultrasonic wave passes through a liquid, formation, growth, and implosive collapse of bubbles occurred [41]. This process has been called cavitation and was rapidly repeated. As a result, the local temperature rises to several thousand Kelvin for a short

time due to the collapse of bubbles [42]. The energy released from this process, would lead to enhanced chemical reactivity and accelerated reaction rates [43]

In this research, we have prepared extremely pure nanocrystallites of $\text{Co}(\text{OH})_2$ and Co_3O_4 with the help of ultrasound irradiation. The optical and structural properties of cobalt hydroxide and oxide investigated by scanning electron microscopy (SEM), X-ray diffraction (XRD) and Uv-Visible spectroscopy.

2. Experimental procedure

2.1. Materials

Cobalt acetate tetrahydrate ($(\text{Co}(\text{CH}_3\text{COO})_2 \cdot 4\text{H}_2\text{O})$, Purity $\geq 99\%$) and sodium hydroxide (NaOH , Purity $\geq 99\%$) were purchased from merck. All of these chemical reagents were used as received without purification.

2.2. Instruments

Morphological and structural investigations were performed using the LEO 1430 VP scanning electron microscope (SEM) whit 14 and 15 kV accelerating voltage. Optical properties were carried out using a UV-Vis spectrophotometer (Shimadzu, model 1650, Japan). The structural characterization of nanocrystals was carried out by analyzing X-ray diffraction (XRD) patterns, obtained using a Philips X Pert, X-raydiffractometer using $\text{Cu K}\alpha$ radiation (wavelength=1.54056 Å).

2.3. Synthesis

The cobalt oxide and cobalt hydroxide nanocrystalline structures in a powder form were prepared by ultrasound-assisted technique. The nanocrystalline cobalt oxide and cobalt hydroxide were grown in aqueous media at normal laboratory conditions. In a typical synthesis of $\text{Co}(\text{OH})_2$ nanoparticles, 0.996g cobalt acetate and 0.16g sodium hydroxide (NaOH) were dissolved in 20ml of distilled water, respectively. The sodium hydroxide solution was then added to the cobalt acetate solution. Then the obtained solution was placed under ultrasonic irradiation for one hour at room temperature in open air, using the Dr. Heisler high intensity ultrasonic processor (200 W/cm^2 , 23 Hz). The final precipitation was washed with distilled water and centrifuged for several times and then the dried powder nanomaterials were used for different techniques.

3. Results and discussion

3.1. TGA

TGA and DTA spectra have been recorded in temperature simultaneous thermal system. A ceramic Al_2O_3 crucible was used for heating and measurements were carried out in N_2 atmosphere at heating rate

$10^\circ\text{C}/\text{min}$. TGA and DTA curves of powder cobalt hydroxide nanopowders are given in figures 1 and 2. It is observed from TGA curve that %17 weight loss of the sample occurred in temperature region between 200°C and 250°C . There is almost no weight loss observed above 250°C . An initial weight loss observed below 200°C , it can be attributed to the evaporation of water. Overall TGA results show a loss of %17 up to 250°C . We also carried out the DTA measurement. Three phases of changes are observed. They are marked with the number (1), (2) and (3). Point 1, refers to water evaporation the sample has 10% weight of water. Point 2 presents a small shoulder corresponding to dehydration of the sample, which is the endothermic process. Point 3 represents the exothermic changes or oxidation and crystallization of the cobalt hydroxide to the cobalt oxide material. DTA curve displays an intense exothermic peak between 210°C and 280°C which attributed to crystallization of cobalt hydroxide nanoparticle.

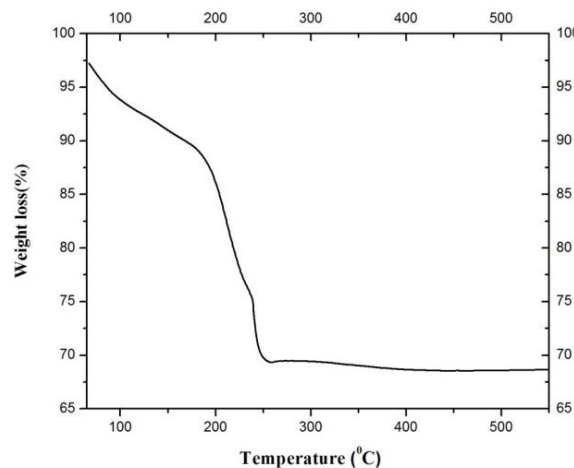


Fig. 1. TGA curve of the cobalt hydroxide nanostructures prepared by ultrasound-assisted method

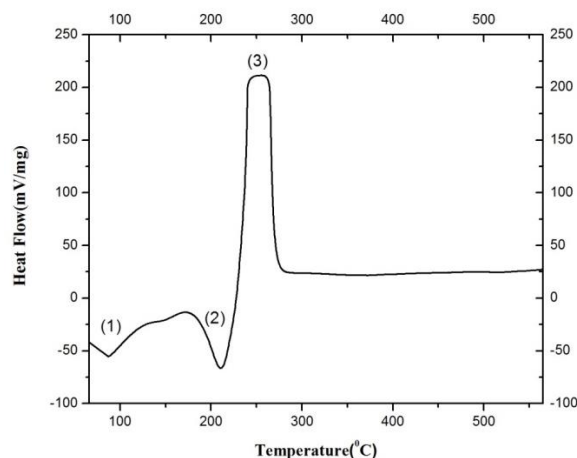


Fig. 2. DTA curve of the cobalt hydroxide nanostructures prepared by ultrasound-assisted method

3.2. Structural studies

The crystallographic characteristics and the phase purity of the product were investigated using X-ray diffraction (XRD). Fig. 3 shows the typical XRD pattern of the as-prepared $\text{Co}(\text{OH})_2$ Nanostructures. It can be observed that all the diffraction peaks could be readily indexed to pure hexagonal phase of Cobalt hydroxide material with space group of P-3m1. (JCPDS card file No. 45-0031). No obvious peaks of impurities were seen in this pattern.

Fig. 4, shows the XRD pattern of the product obtained by heat treatment at 300°C for 1 hour of cobalt hydroxide nanostructures. All the diffraction peaks can index as a cubic phase of cobalt oxide (Co_3O_4) material with a space group of Fd-3m (JCPDS card No. 78-1970). No other impurity peaks are observed in the XRD pattern, indicating the complete transformation of Cobalt hydroxide to Cobalt oxide. All advantage of X-ray diffraction is also that this method provides a very simple possibility for estimating the by means of the so-called Scherrer formula [44]:

$$D = 0.9\lambda / \beta \cos\theta \quad (1)$$

Where, λ is the wavelength of the X-ray ($\sim 1.5414 \text{ \AA}$). θ is the angle of the considered peak, β is a full width at half maximum (FWHM) of the peak and K is a constant close to unity. Nanoparticle sizes have been calculated from the line broadening of XRD diffraction peaks according to the Scherrer formula and listed in table 1 and 2. All calculations confirm that the structures are nanocrystalline in nature with average size below 30nm in The case of both Cobalt hydroxide and oxide materials.

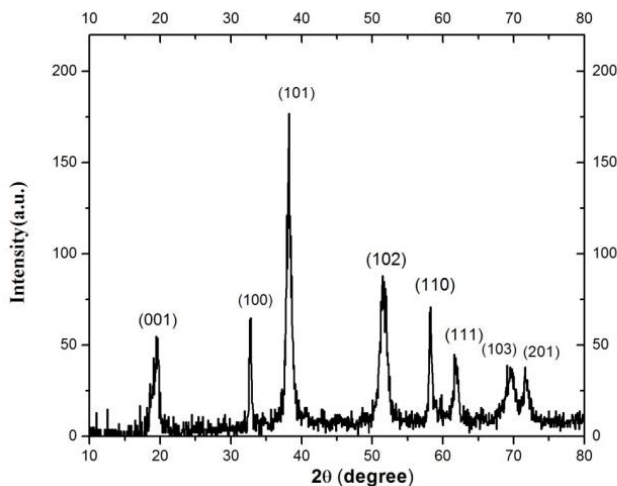


Fig 3. X-ray diffraction pattern of cobalt hydroxide nanostructures prepared by ultrasound-assisted method

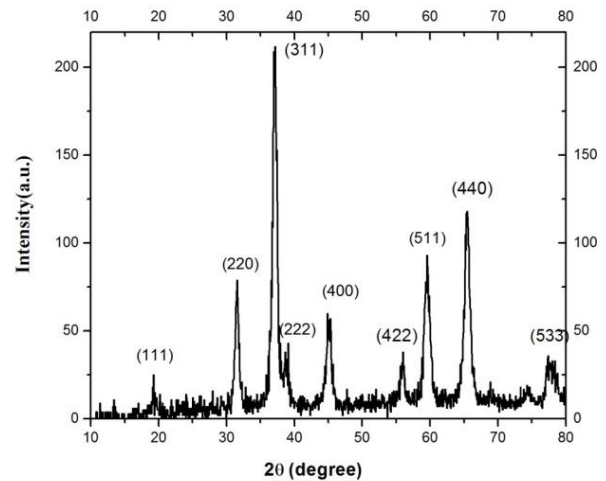


Fig. 4. X-ray diffraction pattern of cobalt oxide nanostructures prepared by ultrasound-assisted method

Table 1. grain size calculated from XRD pattern of cobalt hydroxide

Pos. [$^{\circ}2\theta$.]	FWHM [$^{\circ}2\theta$.]	hkl	$d_{\text{cal}}(\text{nm})$
19.5674	0.4723	(001)	17.3
32.7624	0.2952	(100)	28.2
38.1868	0.5904	(101)	14.4
51.5857	0.9446	(002)	9.4
58.2398	0.3542	(102)	26.1
61.8599	0.7085	(110)	13.2
69.5914	0.9446	(103)	10.3
71.7466	0.8640	(201)	11.4

Table 2. grain size calculated from XRD pattern of cobalt oxide

Pos. [$^{\circ}2\theta$.]	FWHM [$^{\circ}2\theta$.]	hkl	$d_{\text{cal}}(\text{nm})$
19.2297	0.7085	(111)	11.4
31.5316	0.3542	(220)	23.8
37.0805	0.3542	(311)	24.3
38.7306	0.7085	(222)	11.9
45.0952	0.5904	(400)	13.4
55.9418	0.4723	(422)	19.2
59.5215	0.9446	(511)	8.5
65.4563	0.7085	(440)	13.4
77.5089	0.8640	(533)	9.2

3.3. Morphological studies

The morphology of the products has been studied by scanning electron microscope. Figure 5(a) and (b) shows the SEM images of $\text{Co}(\text{OH})_2$ and Co_3O_4 Nanostructures. The SEM images does not show great correlation with the nonocrystal size values calculated using Scherrer formula from XRD data as shown in figure. It is evident that the product consists of agglomeration of nanocrystals and wide distribution of grains with grain size ranging from below 100nm to micrometer distributed nonuniformity.

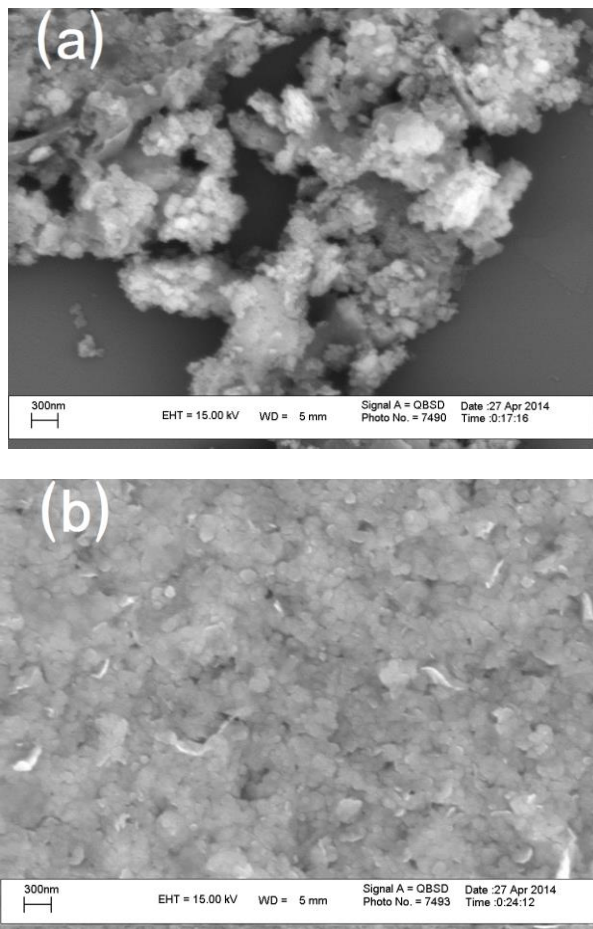


Fig. 5. (a) SEM images of $\text{Co}(\text{OH})_2$ and (b) Co_3O_4 nanostructures prepared by ultrasound-assisted method

3.4. Optical studies

One of the most essential semiconducting parameters is the band-gap energy. In order to obtain the fundamental band-gap energy, we have measured the optical absorption spectra of these compositions. Figs 5 and 6 shows the UV-Visible absorption spectra of the $\text{Co}(\text{OH})_2$ and Co_3O_4 nanoparticles, respectively. The absorption spectrum of Co_3O_4 shows that there are two direct band gaps. The first band can be assigned to the $\text{O}^{2-} \rightarrow \text{Co}^{2+}$ charge transfer process while the second band gap can be assigned to $\text{O}^{2-} \rightarrow \text{Co}^{3+}$ charge transfer process [45].

The band gap value E_g can be calculated from the following equation [46]:

$$(\alpha h\nu)^n = B(h\nu - E_g) \quad (2)$$

Where α is the absorption coefficient, $h\nu$ is the photon energy, B is a constant characteristic to the material, and n equals either 1/2 for an indirect transition or 2 for a direct transition. The variation of $(\alpha h\nu)^2$ in contrast to $h\nu$ is shown in figure 8 and 9. The value of band gap for cobalt hydroxide estimated 2eV and in the absorption spectrum of Co_3O_4 nanoparticles the band gap for $\text{O}^{2-} \rightarrow \text{Co}^{3+}$ transition estimated 1.8 and the band gap for the $\text{O}^{2-} \rightarrow \text{Co}^{2+}$ transitions estimated 3.2eV.

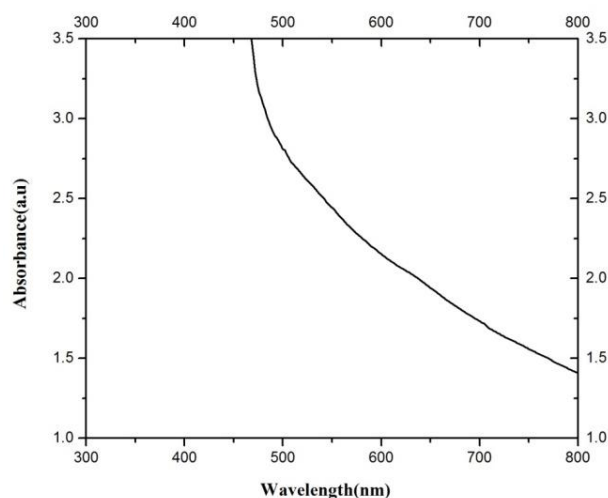


Fig. 6. UV-Visible absorption spectra of cobalt hydroxide nanostructures prepared by ultrasound-assisted method

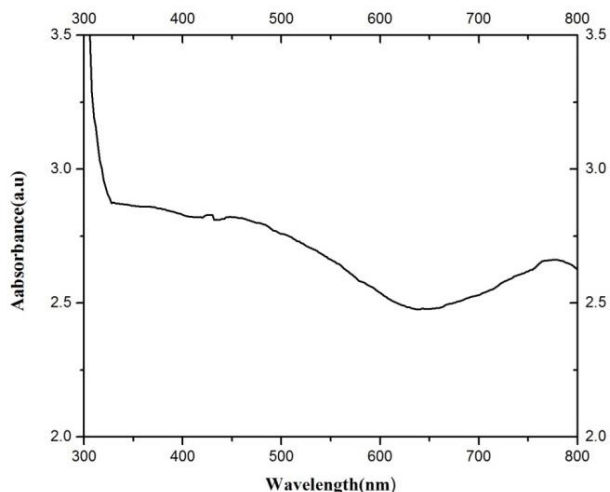


Fig. 7. UV-Visible absorption spectra of cobalt oxide nanostructures prepared by ultrasound-assisted method

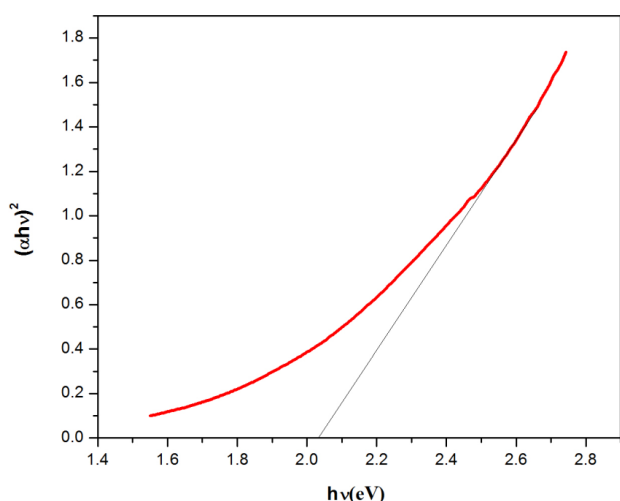


Fig. 8. Determination of the optical band gap from the plots of $(\alpha hv)^2$ versus $h\nu$ for the cobalt hydroxide

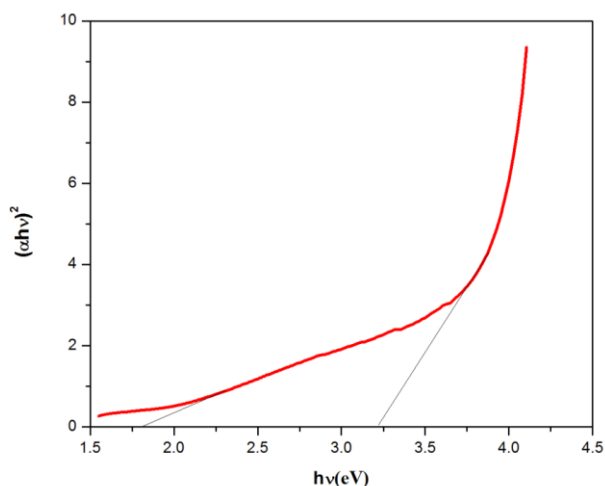


Fig. 9. Determination of the optical band gap from the plots of $(\alpha hv)^2$ versus $h\nu$ for the cobalt oxide

4. Conclusion

In summary, we have studied in detail the structural and optical properties of $\text{Co}(\text{OH})_2$ and Co_3O_4 nanostructures. We have proposed an ultrasound-assisted method for nanostructures grown of high quality and pure $\text{Co}(\text{OH})_2$ and Co_3O_4 , but the product consist of agglomeration of nanocrystals and wide distribution of grains. The optical investigation, TGA and DTA analyses also confirm the formation of cobalt hydroxide and cobalt oxide nanomaterials. The results of XRD pattern shows formation of pure cobalt oxide and cobalt hydroxide compounds with average grain sizes are below 30 nm.

References

[1] P. Eskandari, F. Kazemi, Y. Azizian-Kalanderagh, Separation and Purification Technology **120**, 180 (2013).

- [2] M. R. Hoffman, S. T. Martin, W. Choi, D. W. Bahnemann, Chem. Rev. **95**, 69 (1995).
- [3] Y. Azizian-Kalanderagh, A. Khodayari, Phys. Status Solidi. **A207**, 2144 (2010).
- [4] B. Ozpineci, L. M. Tolbert, ORNL.TM. **257** (2003).
- [5] P. V. Kamat, J. Phys. Chem. C **112**, 18737 (2008).
- [6] M. A. Fardad, J. Mater. Sci. **35**, 1835 (2000).
- [7] S. A. Makhlof, J. Magn. Mater. **246**, 184 (2002).
- [8] L. Gong, L. Su, Appl. Surf. Sci. **257**, 10201 (2011).
- [9] T. Zhao, H. Jiang, J. Ma, J. Power Sour. **196**, 860 (2011).
- [10] R. M. A. Lieth, Kluwer Academic Publisher, Dordrecht (1997).
- [11] S. L. Chou, J.-Z. Wang, H. K. Liu, S. X. Dou, J. Electrochem. Soc. **155**, 926 (2008).
- [12] M. Dinamani, P. V. Kamath, App. Electrochem. **30**, 1157 (2010).
- [13] M. Vidotti, C. van Greco, E. A. Ponzio, S. I. Córdoba de Torresi, Electrochem. Commun. **8**, 554 (2006).
- [14] M. Behazin, M. C. Biesinger, J. J. Noel, J. C. Wren, Corrosion. Sci. **63**, 40 (2012).
- [15] C. W. Tang, C. B. Wang, S. H. Chien, Thermochemica. Acta. **473**, 68 (2008).
- [16] H. Yamaura, K. Moriya, N. Miura, N. Yamazoe, Sens. Actuators B **65**, 39 (2000).
- [17] R. Van Zee, Y. Hamrick, S. Li, W. Weltner, J. Phys. Chem. **96**, 7247 (1992).
- [18] C. B. Wang, H. K. Lin, C. W. Tang, Catal. Lett. **94**, 69 (2004).
- [19] Ch. W. Tang, Ch. B. Wang, Sh. H. Chien, Thermochemical Acta **473**, 68 (2008).
- [20] C. Mocuta, A. Barbier, G. Renaud, Appl. Surf. Sci. **56**, 162 (2002).
- [21] L. Bornstein, Physics of Nontetrahedrally Bonded Binary Compounds, 17, Springer, New York (1984).
- [22] S. Katalin, G. Szabo, M. Zrinyi, J. Nanosci. Nanotechnol. **11**, 1 (2011).
- [23] Q. Yuanchun, Z. Yanbao, W. Zhinshen, Mater. Chem. Phys. **457**, 110 (2008).
- [24] M. Koinuma, T. Hirae, Y. Mutsomoto, J. Mater. Res. **13**, 837 (1998).
- [25] J. Jansson, A. E. C. Palmqvist, E. Fridell, J. Katal. **211**, 387 (2002).
- [26] S. D. Choi, B. K. Min, Sens. Actuators, B **77**, 330 (2001).
- [27] S. A. Makhlof, J. Magn. Mater. **246**, 184 (2002).
- [28] M. G. Hutchins, P. J. Wright, P. D. Grebenic, Solar Energy Mater. **16**, 113 (1987).
- [29] F. Svegl, B. Orel, I. Grabec-Svegl, V. Kaueie, Electrochim. Acta. **45**, 4359 (2000).
- [30] N. Koshizaki, N. Yasumoto, T. Sasaki, Sens. Actuators B. Chem. **66**, 122 (2000).
- [31] R. H. Kodama, J. Magn. Mater. **200**, 359 (1999).
- [32] M. Ghosh, E. V. Sampathkumaran, C. N. R. Rao, Chem. Mater. **17**, 2348 (2005).
- [33] L. Bornstein, Physics of Nontetrahedrally Bonded Binary Compounds, 17, Springer, New York (1984).
- [34] P. Gupta, M. Ramrakhiani, The Open Nanoscience Journal **3**, 15 (2009).

- [35] S. Mondal, K. P. Kanta, C. R. Mitra, *J. Phy. Sci.* **12**, 221 (2008).
- [36] S. Katalin, G. Szabo, M. Zrinyi, *Nanosci. Nanotech.* **11**, 1 (2011).
- [37] M. Sathupunya, E. Gulari, A. Jamison, S. Wongkasemjit, *Microporous and Mesoporous Materials* **69**, 157(2004).
- [38] G. Lakshmi, B. B. CHE, C. R. Martin, E. R. Fisher, *Cem. mater.* **10**, 260 (1998).
- [39] Y. T. Chen, W. Q. Zhang, Y. Fan, X. Xu, Z. X. Zhang, *Mater. Chem. Phys.* **98**, 191 (2006).
- [40] V. Saez, Timothy J. Mason. *Molecules* **14**, 4284 (2009).
- [41] K. Suslick, *Mater. Res. BULL.* **29**, 4 (1995).
- [42] J. Lorimer, T. Mason, *Chem. Soc. Rev.* **239**, 16 (1987).
- [43] K. S. Suslick, *Ultrasound: its chemical, physical, and biological effects.* New York: VCH Publishers (1988).
- [44] C. W. Tang, C. B. Wang, S. H. Chien, *Thermochimica Acta* **473**, 68 (2008).
- [45] A. Gulino, P. Dapporto, P. Rossi, I. Fragala, *Chem. Mater.* **15**, 3748 (2003).
- [46] X. Wang, X. Chen, L. Gao, H. Zheng, Z. Zhang, Y. Qian, *J. Phys. Chem. B* **108**, 16401(2004).

*Corresponding author: azizian@uma.ac.ir,
yashar.a.k@gmail.com